

SEVENTEENTH EUROPEAN ROTORCRAFT FORUM

Paper No 91 - 48

**A STUDY OF HELICOPTER ROTOR/FUSELAGE RESPONSE IN
LOW-SPEED MANOEUVRES : COMPARISON
OF THEORY WITH FLIGHT**

A T McCALLUM

**DEFENCE RESEARCH AGENCY
(AEROSPACE DIVISION)
RAE BEDFORD
UK
MK41 6AE**

SEPTEMBER 24 - 26, 1991

Berlin, Germany

**Deutsche Gesellschaft für Luft- und Raumfahrt e.V. (DGLR)
Godesberger Allee 70, 5300 Bonn 2, Germany**

OPGENOMEN IN
GEAUTOMATISEERDE
CATALOGUS

1061317

**A STUDY OF HELICOPTER ROTOR/FUSELAGE RESPONSE IN
LOW-SPEED MANOEUVRES : COMPARISON
OF THEORY WITH FLIGHT**

**A T McCALLUM
DEFENCE RESEARCH AGENCY
(AEROSPACE DIVISION)
RAE BEDFORD
UK**

Summary

Comparisons have been made of the behaviour of a rigid blade rotor simulation model with data gathered on a Puma helicopter during quick-hop manoeuvres as part of a validation study. Two validation techniques are investigated; the first method involves driving a full helicopter simulation model with pilot controls, whilst the second involves driving an isolated rotor model with rotor controls and fuselage motions. Relative merits of each method are discussed and, in the case of the quick-hop manoeuvre, the advantages of using the latter method, called open loop simulation, are demonstrated. Inflow dynamics and nonlinear section aerodynamics are briefly discussed and preliminary results illustrating the effects of these modelling features presented. It is concluded that the method of driving open loop simulation is ideal for validating and understanding rotor behaviour and will be investigated for a broader range of flight conditions and rotor system types.

1 Introduction and Background

Mathematical modelling of helicopter flight mechanics and aerodynamics are active areas of research at the Defence Research Agency (formerly the Royal Aerospace Establishment), Bedford. To date this work has involved both the development of theoretical models of rotor and other vehicle components and the gathering and analysis of flight test data. Current flight test programmes are concerned with the detailed measurement of main rotor aeroelastic response (Ref 1) and the aerodynamic field around the tail rotor of the Bedford Lynx aircraft (Ref 2).

Until recently, the flight mechanics modelling work performed at Bedford has been centred around the Helistab model (Ref 3) and Helisim, its real-time implementation. Current applications of these models are the design of advanced control laws, studies of handling qualities of military helicopters and the assessment of novel helicopter types. Helistab is an off-line program while Helisim operates within the framework of the control laws design package TSIM (Ref 4).

With fly-by-wire and actively controlled rotorcraft now under development (eg RAH-66, V-22, NH-90), the need to simulate vehicle behaviour at, or close to, the flight envelope limits, is stronger than ever before and requires a more rigorous approach to the modelling of vehicle dynamic and aerodynamic response. In particular, many models of the main rotor (including Helistab) incorporate assumptions which break down beyond the regime of 'normal' flight. Examples of this are the modelling of rotor blades as rigid bodies, the exclusion of flow separation and compressibility effects and simple momentum formulations for inflow.

To address and, where possible, redress these limitations a programme of work is now underway at DRA Bedford to develop a generic aeroelastic rotor model (Ref 5) intended to replace the Helistab family and to meet future requirements for the next 5 - 10 years. In parallel to the formulation and development of the aeroelastic model is a study to examine and develop appropriate methods of model validation. This paper compares two possible candidates. The first, referred to as the 'closed loop' method (Ref 6) involves motivating the simulation model of the entire vehicle with main- and tail-rotor control deflections measured in flight. In the second method, referred to as 'open loop' simulation, a model of the main rotor is driven by the main rotor controls and fuselage translational and angular velocities.

The study described in this paper applies these methods to the Helistab model and to a simple blade element rotor model, respectively. Model enhancements are easily implemented in the blade element model and the inclusion of the Pitt and Peters dynamic inflow model (Ref 7) and lookup tables of blade section aerodynamic properties are examined.

Comparisons are made between the rotor model response, characterised by time histories of multiblade coordinates and thrust coefficient, with those reconstructed from flight data gathered on the Puma for hover and low speed manoeuvres. In particular, quick-hop test cases are examined and comparisons of the rotor model and the full Helistab simulation made. The results of the open loop simulation are very promising and the technique offers real benefits to the validation of rotor models. Areas for future work are discussed and expansions of the open loop method suggested, which could assist the validation of full vehicle simulations.

2 Flight Test Data and Analysis

Until late 1989, the primary flight mechanics research aircraft used at DRA Bedford was a comprehensively instrumented Aerospatiale SA300 Puma (Fig 1). In this aircraft the fuselage motion was measured by rate and attitude gyros and accelerometers mounted in selected locations with aerodynamic velocities, sideslip and angle of attack measured, respectively, by a pitot head and vanes mounted on a probe extending from the nose of the aircraft. Pilot control deflections and basic articulated rotor degrees of flap, lag and feather measured

by potentiometers. Rotor data were passed through a slip-ring assembly to the MODAS (Modular Data Acquisition System) onboard data recording system. Reference blade azimuth angle was measured by an optical pick-off device in the base of the slip-ring assembly. In-flight measurements were recorded onto tape by the MODAS system and later downloaded through an off-line replay system to produce computer compatible tapes.

During a ten month period extending from November 1987 until September 1988, the Puma was used to perform a series of flight tests in support of the General Purpose Research Instrumented Blade (GPRIB) programme. This research programme, described in detail in Reference 8, was concerned with the measurement of aerodynamic behaviour of the main rotor using a set of blades fitted with pressure sensors at selected spanwise and chordwise locations. Most of the flights performed for the GPRIB programme involved steady hover or forward flight cases with manoeuvring flight restricted to roll reversals and turning manoeuvres at relatively high forward velocity. However, late in the programme a limited series of mission task elements (MTEs) were flown with the full instrumentation engaged, allowing analysis of aerodynamic behaviour to be made for the transition from hover to low-speed forward- and sideways flight.

Included in the set of MTEs was a set of quick-hop manoeuvres, a typical profile of which is illustrated in Figure 2. The quick-hop can be characterised by two parameters; the initial 'pitch-down' attitude and total ground distance to be covered. Test observer's data shows that three quick-hops were performed at 10° , 20° and 30° of pitch down. Thus three levels of 'aggression' were recorded for the manoeuvre of interest and based on an 'eyeball' analysis of the quick-hop data the largest of these (Event 19) was chosen for initial analysis.

RIBAN (Research Instrumented Blade ANalysis), a special purpose software package (Ref 8), uses the data measured from the GPRIB pressure sensors in the reconstruction of the local aerodynamic incidence and normal loading around the main rotor. Two typical RIBAN outputs, a polar plot of normal force coefficient for one revolution of the pressure instrumented blade and a spanwise plot of normal force coefficient at a particular azimuthal station are given in Figure 3. It should be noted that the polar plots are normally produced in colour and are therefore more easy to interpret than is suggested by the monochrome example in Figure 3. Prerequisite data for the RIBAN package includes the azimuth angle of the instrumented blade, as the package assumes that the blade is constrained to flap motion only, and the 'aerodynamic' fuselage velocities u , v , w , p , q and r . Corrected azimuth is estimated by RIBAN every revolution of the main rotor by subtracting the lag angle of the instrumented blade from the reference blade position (Fig 4). Individual blade measurements, combined with the corrected azimuth trace, can be used to reconstruct sets of multiblade coordinates of main rotor flapping, lagging and the collective and cyclic pitch applied at the hub.

In the hover, the provision of u , v and w presents a problem as the Puma incidence and sideslip vanes are immersed in the main rotor wake and cannot be

used to measure aerodynamic velocities of the fuselage. KINEMOD, a package developed for checking the kinematic consistency of measured flight data (Ref 9) was, in this case, used to integrate the Euler equations for the helicopter fuselage and estimate from accelerometer data the time histories of u , v , and w . In the hover, any bias errors in the accelerometer readings become immediately apparent by the ramping of body velocities which should be close to zero. Once calculated, the bias errors are easily removed from the velocity traces and corrected and uncorrected traces for part of Event 19 are given in Figure 5. It should be emphasised that the full consistency checks available in KINEMOD were not performed as part of this study.

Figure 6 shows the control input and fuselage time histories for the first 6 seconds of the manoeuvre.

3 Validation Methods

Traditionally, the validation of flight mechanics models has commenced with the process of driving a full vehicle simulation with pilot or actuator controls recorded from flight test. In Reference 6 this is termed 'closed loop' simulation since the forces and moments generated by model 'subsystems' (main rotor, tail rotor, tailplane etc) feed back into the fuselage equations of motion. In this method, small modelling errors are integrated over time and can lead to large deviations of the simulated response from that recorded in flight. Comparison of time history or frequency response data infers where the model may be structurally or parametrically deficient. The use of the word 'infers' is quite deliberate as the interactions between model subsystems contaminate the simulated response and the relations between 'causes' and 'effects' become obscured. This is not to say that 'closed loop' simulation is a fundamentally wrong approach and one only has to look to the literature on system identification and simulation to recognise the usefulness of this approach. As an example, the recent work of Houston (Refs 10 and 11) examined the frequency domain identification of heave axis dynamics for the Puma. In that study, considerable improvements in model response were achieved through a judicious choice of model structure and the introduction of correction factors on specific model parameters. Figure 7 (taken from Ref 10) shows the correlation between the enhanced model and flight data for a bob-up and remask manoeuvre. The success of this heave dynamics study can, in part, be attributed to the relatively simple model employed, and its restriction to the heave acceleration, rotor coning and uniform component of dynamic inflow. While the analysis identified an accurate three degrees-of-freedom heave model, valid to around 30 rad/s, identified parameter distortions relative to simple disc/inflow theory were relatively high ($\approx 30\%$) indicating model structure deficiencies.

Alternatives to the closed loop simulation method involve prescribing the flight path of the vehicle and assessing the response of the subsystems to this imposed motion. Reference 6 terms this 'open loop' simulation and in contrast to the 'closed loop' case, the forces and moments generated by the model components are not fed back to influence the overall vehicle response. Du Val,

in Reference 12, likens this method of simulation to operating the mathematical model in a 'wind-tunnel' mode and presents results of a parameter identification exercise using open loop simulation of an AH-64 helicopter. The proposed advantage of this method is that the removal of interactional effects inherent in the model make 'causes' and 'effects' more visible and, once isolated, particular subsystems satisfactorily validated, replaced or enhanced. Another possible validation method which uses a prescribed flight path is the method of inverse solutions which has been applied to a variety of helicopter problems by researchers at the University of Glasgow (Ref 13). In this case the flight path of the helicopter is specified and the constrained vehicle equations of motion solved algebraically to produce time histories of the control deflections and loads required to achieve the prescribed flight path. This can be regarded as a particular application of open loop validation.

In the study documented here, both the closed loop and open loop techniques were applied and assessed. For the closed loop case the full Helistab simulation model was driven by control angles reconstructed from the main rotor blade feathering angles. In the open loop case only the main rotor model was retained and this was driven by both the reconstructed controls and the flight recorded motion of the vehicle, transformed into an axis set centred at the hub. The development of the mathematical models used is discussed briefly in the next section.

4 Theoretical Modelling

Both of the mathematical models used in this study are based on the same formulation of rotor blade motion and can be found in more detail in Reference 3. The formulation assumes that the rotor blade can be represented as a rigid body rotating with angular velocity Ω about the rotor shaft, and is free to flap with angle β about a hinge at the hub centre. It further assumes that the flapping motion is constrained by a spring and the analysis in Reference 3 demonstrates that careful selection of the spring stiffness allows this basic model structure to be used in simulations of rotors with significant real or equivalent hinge offsets.

Based on these assumptions (and again from Reference 3) the equation of motion of blade flapping can be written in non-dimensional form as :-

$$\ddot{\beta}_i + \lambda_{\beta}^2 \beta_i = 2((p_w + q_w)\cos\psi_i - (q_w - p_w)\sin\psi_i) + M_{\beta i} \quad [1]$$

where p_w and q_w are the non-dimensional fuselage roll and pitch rates in rotor wind axes, ψ_i is the azimuth angle of the i^{th} blade, $M_{\beta i}$ is the aerodynamic moment on the blade about the flapping hinge and $(\dot{})$ denotes differentiation with respect to ψ_i .

In Reference 3 an analytic expression for $M_{\beta i}$ is derived and involves terms in the hub referenced velocities u_h , v_h and w_h , rates q_w and p_w , applied blade pitch θ_p , linear blade twist rate θ_{tw} and inflow components λ_0 , λ_{1s} and λ_{1c} . Applying the multiblade transformation to the flapping motion,

$$\beta_0 = \frac{1}{N} \sum_i \beta_i \quad [2a]$$

$$\beta_{1s} = \frac{2}{N} \sum_i \beta_i \sin(\gamma_i) \quad [2b]$$

$$\beta_{1c} = \frac{2}{N} \sum_i \beta_i \cos(\gamma_i) \quad i = 1..N \quad [2c]$$

yields the Helistab disk representation of rotor blade flapping.

Hub referenced velocities are obtained from fuselage referenced velocities through the transformation

$$\begin{bmatrix} u_h \\ v_h \\ w_h \end{bmatrix} = \begin{bmatrix} \cos(\gamma_s) & \sin(\gamma_s) \\ 0 & 1 & 0 \\ -\sin(\gamma_s) & \cos(\gamma_s) \end{bmatrix} \begin{bmatrix} u_A - q \cdot h_{rr} \\ v_A + p \cdot h_{rr} + r \cdot x_{cg} \\ w_A - q \cdot x_{cg} \end{bmatrix} \quad [3]$$

where γ_s is the shaft tilt angle, h_{rr} is the height of the rotor hub centre above the aircraft centre of gravity and x_{cg} is the rearwards distance from the cg to the Helistab reference point.

For the individual blade rotor model, equation [1] is used directly and the aerodynamic moment $M_{\beta i}$ calculated numerically in two different ways. The first of these embodies the Helistab assumption that the aerodynamic velocity normal to the plane of rotation of the blade (U_N) is substantially smaller than the in-plane component (U_T) and is calculated from

$$M_{\beta i} = \frac{1}{2} \gamma \int_0^1 (U_T^2 \theta + U_N U_T) r dr \quad [4]$$

where θ includes applied pitch and blade twist, r is the distance of the blade section from the hub centre, normalised by main rotor radius and γ is the main rotor Lock number.

In the second case no assumptions are made about the relative magnitudes of U_N and U_T and nonlinearity is introduced in the form of lookup tables of section aerodynamic properties derived from wind tunnel tests and corrected for Mach number effects. In this case the aerodynamic moment is calculated from

$$M_{Bi} = \frac{\frac{1}{2} \rho c}{I_B} \int_0^1 U_{tot}^2 (C_L \cos(\phi) + C_D \sin(\phi)) r dr \quad [5]$$

where the inflow angle $\phi = \arctan(U_N/U_T)$, $C_L = C_L(\alpha, M)$, $C_D = C_D(\alpha, M)$, ρ is the local air density, c is the aerodynamic chord, U_{tot} is the total velocity at the blade section and I_B is the blade second moment of mass about the flapping hinge.

Spanwise Integration is performed numerically over a variable number of elements up to a maximum of one hundred. For all of this study eight elements of equal length were used.

Figure 8 shows schematically the process of taking flight data from the aircraft and using it to drive each of the models described above.

In Helistab, inflow is included in the classical Glauert quasi-steady form of,

$$\lambda_0 = \frac{C_T}{2\sqrt{\mu^2 + (\mu_z - \lambda_0)^2}} \quad [6]$$

which is solved iteratively at every time step using Newton's method. This basic model was included in the blade element model but an alternative in the form of the Peters-HaQuang modification (Ref 14) to the Pitt-Peters model was included. This model has the structure,

$$[M] \{\dot{\lambda}\} + [V][L_B]^{-1} \{\lambda\} = \{C\} \quad [7]$$

where $[M]$ is the matrix of apparent mass terms,

$[V]$ is a 'blending' matrix which shapes the inflow response during transition from hover to forward flight,

$[L_B]$ is the static gains matrix transformed from wind axes to shaft axes,

$\{\lambda\} (= \{\lambda_0 \ \lambda_{1s} \ \lambda_{1c}\}^T)$ is the vector of inflow components,

and $\{C\}$ ($= \{C_T \ C_L \ C_M\}^T$) is the vector of thrust, rolling moment and pitching moment coefficients.

Apart from the model structure defined above a number of assumptions need to be highlighted. Firstly, for these initial comparisons, rotor speed is assumed to be constant and the impact of this assumption is discussed later. Secondly, the flight trials were conducted in partial ground effect and no attempt has been made to model the corresponding inflow distortions during the manoeuvres, but it is recognised that they are potentially significant and the effects will be considered in future work.

5 Comparison of Theory with Flight

Closed Loop Simulation

Figure 9 shows the fuselage linear and angular velocities which result from driving Helistab with reconstructed control inputs for the first 6 seconds of the quick-hop manoeuvre in Event 19. It is fairly obvious from the figure that, for this particular manoeuvre, the response of the closed loop simulation rapidly diverges from that observed in flight, particularly in the case of yaw rate and sideslip velocity. However, the 'on axis' responses of pitch rate, q , heave velocity, w and forward velocity, u , correlate fairly well with flight for 2 - 3 seconds after initiation of the manoeuvre.

Considering the main rotor response, Figure 10 compares the multiblade coordinate time histories for Helistab with those reconstructed from flight. The Helistab results have been corrected to have the same trim values as the flight data and Table 1 compares the actual trim values for all the Event 19 runs performed in this study. It should be noted that the high frequency 'chatter' on the flight data between 3.5 - 4 seconds is attributed to the measured flap angle signals saturating at -4° and $+8^\circ$ degrees.

Overall the results for the main rotor present a similar pattern to those for the fuselage rates, with the on-axis response for β_{1c} correlating reasonably with the flight data for 2 - 3 seconds after pilot input. Coning angle β_0 exhibits an overshoot 50% higher than in flight and, towards the end of the run, starts to wash off, matching the flight data at around 5 - 6 seconds. While similar trends to this can be seen in the body rates it is suggested that the heave velocity, w , is contributing most to this decay through its influence on the induced flow velocity as given in equation [6]. Lateral flap, β_{1s} , is small in comparison to the other flapping coordinates and, similar to the longitudinal flap, matches well with the flight trace.

Open Loop Simulation

In the open loop case the principal outputs available for comparison are the multiblade coordinates calculated from the individual blade responses in the

blade element model. Figure 11 shows these overplotted with the Helistab results and the flight data reconstructions. In this case the model is configured to use Glauert inflow and numerically integrated loads calculated according to equation [4]. As the model is effectively the same as that in Helistab, the trim collective setting was chosen to be that calculated by Helistab, with the flight data collective used as a perturbation on this value. As with the Helistab runs, the multiblade coordinates from the blade element model have been corrected to have the same trim values as those observed in flight.

As would be expected from essentially identical rotor models, the initial response of the open loop simulation to pilot's control is very similar to the closed loop simulation, with, for example, a very similar overshoot in coning. Beyond the first one or two seconds however, it is apparent from the coning trace that the open loop simulation, although offset, is following the flight data more faithfully and for further into the run. However, β_{1s} and β_{1c} both correlate well with the flight data, diverging little over the run.

Running the open loop simulation using the Pitt-Peters dynamic inflow model does give some improvement, evident from the reduction in overshoot in β_{1c} (Fig 12). Similarly, β_0 exhibits a slight increase in overshoot and reduction of 'steady state' response which would be expected when inflow dynamics are present. The inclusion of the Pitt-Peters model would appear to be qualitatively beneficial. Lateral flap, β_{1s} , diverges slightly towards the end of the run and looking at the time histories for the inflow components (Fig 13) it can be seen that λ_{1s} and λ_{1c} behave similarly. It should be noted that the uniform component of inflow and thrust coefficient time histories for both models are practically identical, as might be expected. It is no surprise that the λ_{1s} component calculated by the Glauert model is markedly different from that resulting from the Pitt-Peters model since, in the Glauert model, it occurs only as a function of the rotor sideslip angle, whereas the Pitt-Peters models treats it as an independent degree of freedom.

To test the repeatability of these results the open loop simulation was run for the first seven seconds of Event 18, another quick-hop manoeuvre with an initial 'pitch down' of 20° . The results of this exercise are shown in Figure 14 where comparisons are made of the simulated and flight derived multiblade coordinates. Again, the open loop simulation time histories compare well with those recorded in flight and once more the presence of inflow dynamics has a favourable influence. Unlike Event 19, where the coning exhibited the greatest overshoot, it is the on-axis longitudinal flapping, β_{1c} , which is now overpredicted most by the simulation.

As a means of examining more fully the potential benefits of open loop simulation, the rotor model was driven with the full 22 seconds of data available for Event 19. Figure 15 shows time histories of control inputs and fuselage rates for the full run and the traces for u and q illustrate well the phases of the quick-hop shown earlier in Figure 2. As shown in Figure 16, the results of an initial run with Glauert inflow and no Mach correction are very promising and

the fact that no divergence occurs between the simulation results and flight measurements over such a long period is, in itself, an encouraging result. As before, Figure 16 illustrates that the β_0 response is overpredicted by theory although closer inspection shows that much of the higher frequency 'fine' detail is fairly well predicted and the overall 'shape' of the response agrees favourably with the flight data. Longitudinal flap follows the flight data fairly faithfully, apart from the pitch reversal phase of the manoeuvre where a significant offset is observed. However, for the final 8 seconds of the flight, including the deceleration and return to hover, the match is exceptionally good. Lateral flap is similarly faithful over much of the run except for the portion between 12 and 16 seconds where the simulation response has a 'shape' and magnitude similar to the flight data but a positive bias of about two degrees.

It should be realised that the quick-hop manoeuvre represents a particularly severe test for rotor modelling with the thrust, torque and control deflections varying across a wide range of operating conditions from high thrust to near-autorotative states. Unmodelled effects are undoubtedly more significant in some phases. Figure 17 illustrates the rotor speed variations during Event 19 with an 8% peak to peak change, highlighted by the droop at 15 seconds as collective pitch is pulled in during the recovery to the hover. In addition, the manoeuvre takes place in close proximity to the ground and it may be that this is contributing effects which immediately limit the applicability of the chosen model structure.

Figure 18 compares the multiblade coordinate responses of the open loop simulation using Glauert inflow and simple numerical loads (using equation [4]) with the responses generated from a run using Pitt-Peters dynamic inflow and Mach corrected numerically integrated loads (equation [5]). It is obvious that the look-up table data increases the level of perturbation in all responses. This may be due in part to the use of NACA 0012 tables, which is not strictly the correct aerofoil for the Puma where the blade section is closer to NACA 0011. It should be noted that the *Helistab* value of lift curve slope is 5.73 where the lowest value in the lookup tables is around 6.3 representing a variation of $\approx 10\%$. Generally, however, the time responses for the Mach corrected, dynamic inflow case are qualitatively similar to those for the linear aerodynamic, Glauert inflow model. It would appear from this that, in this example, the addition of a more complex representation of blade section aerodynamics has made little difference to the overall model response, indicating a breakdown of other assumptions within the chosen model structure.

Discussion

Although the comparative results and interpretation presented above are tentative, they raise several points of interest which are relevant to areas other than rotor modelling.

Firstly, the closed loop simulation results predict an overall aircraft response which is unrepresentative of the real aircraft with some states, notably

sway velocity v and yaw rate r , being in error both in magnitude and direction. In a flight simulator with motion system, divergence to this extent would almost definitely provide the pilot with false cues and it is possible that the control action required to correct the simulation response would, for example, result in degraded handling qualities ratings for a particular task and thus experimental results unrepresentative of real flight.

Secondly, for the cases considered the closed loop simulation technique has done little more than predict an initial response to a perturbation in the pilot controls. It would be very difficult, based on these results, to select with confidence the model component which is responsible for the rapid divergence. Furthermore, the remainder of the flight data (≈ 15 seconds) is rendered virtually worthless as no useful comparisons can be made during areas of key interest, such as the pitch reversal and deceleration phases of the quick-hop. Phases such as these are of particular interest to the flight mechanics modeller as, in the case of the quick-hop, the rapid change in flight state from accelerating to decelerating forward flight involves transition of the main rotor from high thrust helicopter mode to near autorotation mode. A model of inflow behaviour under these circumstances would not be easily verified or validated if the closed loop method were adopted.

The open loop technique, on the other hand, offers a means of exploring model behaviour not afforded by closed loop simulation. Supported by the results shown in Figure 16 the conclusion can be drawn that the method offers a broader scope for exercising both rotor and inflow models and, almost as a by-product of the manoeuvres chosen here, studying their behaviour during relatively large perturbations in controls and fuselage motions. An additional benefit of open loop simulation is the greater exploitation of flight data, with 22 seconds of useful comparison made for the open loop case as opposed to 2 or 3 seconds for the closed loop case. Flight test data is an expensive commodity and, in this respect, the open loop method offers greater cost-effectiveness. The ability to drive the model with prescribed data does not limit the analysis to comparison with flight data as wind tunnel data could equally be used for comparison. Indeed, comparison of data gathered in the 'clinical' wind tunnel environment with that recorded in flight could prove valuable in developing models of rotor-fuselage interactional aerodynamics.

Open loop simulation has provided qualitative confirmation that dynamic inflow does indeed improve the correlation between simulated and flight recorded rotor responses, although these results are not intended to be definitive and will be subject to further study. However, the large deviations in coning response may indicate poor prediction of the uniform component of inflow, possibly due to the proximity to the ground. It is suggested here that investigation and modelling of physical phenomena such as flight in ground effect is made more straightforward using the open loop method, as a series of models can be run with absolute repeatability of input.

Neither of the methods need be used in isolation and the open loop technique provides a rational approach to the physical validation of model components as part of the task of assembling a fully validated, non-divergent, closed loop simulation. Indeed, the closed loop method needs to be able to work in order to permit piloted simulation studies to proceed. Combining the two techniques could involve the generation of rotor loads time histories from open loop simulation or for that matter flight data and using these to drive the full vehicle model. This would form the basis of a structured validation process.

6 Conclusions

This paper has presented results on the validation of a blade element rotor model using flight test data gathered on the DRA flight research Puma. The test data, selected from a series of low speed mission task elements, has been described and the rotor model theory summarised. Nonlinear blade section aerodynamics and dynamic inflow are two of the features addressed in the validation study. The techniques of closed and open loop simulation validation have been used to achieve greater insight into the modelling strengths and weaknesses.

Closed loop simulation is a well established technique of validating mathematical models of helicopter flight mechanics. Whilst its application has been used successfully for specific flight cases the fact that modelling errors are inevitably present results in the integrated loads, and hence aircraft motion, diverging, in some cases rapidly, from those recorded in flight. This severely restricts the ability of the flight mechanics modeller to assess enhancements to components of the full simulation model. This result has been clearly demonstrated by the divergent responses found in the quick-hop MTE.

This study has examined an alternative method, open loop simulation, and applied it to the validation of a helicopter blade element rotor model. Essential to this method is the availability of high quality flight test data in order that the rotor model may be examined in isolation from the rest of the aircraft. Initial results of this method applied to a quick-hop manoeuvre show that modelling enhancements are easily implemented and their effect on the simulation can be explored more fully than by the closed loop technique. Rapid assessment of modelling subsystems is made possible and flight data utilisation increased significantly. The addition of a dynamic inflow model has been shown to improve the simulation response.

Overall, the results of this initial study are very encouraging, particularly in the primary longitudinal flapping response where flight and simulation agree well. Lateral flapping and coning responses reveal greater excursions in the simulation model and further model validation work is required to explain these features.

7 Future Work

Much work needs to be done to improve the theoretical rotor model used in the open loop simulation and in particular the addition of currently unmodelled dynamics such as rotorspeed and lag. Further expansion of the blade element representation is also required with the inclusion of spanwise variations in mass, chord, twist and aerodynamic section. The aeroelastic model currently under development (Ref 5) meets all these requirements.

Dynamic inflow has been briefly explored during the study but much more work needs to be done. In particular, alternatives to the Pitt-Peters model will be explored as will the effects of ground proximity on inflow discussed by Chen in his inflow review paper (Ref 15).

Examination of different flight cases and rotor system types is essential. In particular the heave axis response in hover will be revisited to compare results of this method with Houston's identification work. The open loop method could prove to be useful in system identification studies and it will certainly be used to assess the influence and significance of rotor aeroelastic modes in the new full envelope aeroelastic model. Data gathered during the Lynx flight test program described in Reference 1 will play an invaluable role in exploiting this technique.

Acknowledgements

The author would like to express his gratitude to colleagues in the Helicopter Aeromechanics Section, DRA (Bedford) for their support and assistance during this project. Particular thanks are due to Graham Turner and Christian Sugrue for their invaluable help in preparing and presenting flight test data and Helistab results. Thanks also to Dr Gareth Padfield for his advice and encouragement.

References

1. P C Tarttelin, Rotor Aeromechanics Research with the RAE Research Lynx, **Proceedings of the 16th European Rotorcraft Forum**, Paper No II.7.4, Glasgow, Scotland. Sept 1990
2. Lt A D S Ellin, RN, Tail Rotor Aerodynamic Features Recorded in Flight, **Proceedings of the 16th European Rotorcraft Forum**, Paper No I.4.4, Glasgow, Scotland. Sept 1990
3. G D Padfield, A Theoretical Model of Helicopter Flight Mechanics for Application to Piloted Simulation, **RAE Technical Report TR 81048**, April 1981
4. J S Winter, M J Corbin and L M Murphy, Description of TSIM2: A Software Package for Computer Aided Design of Flight Control Systems, **RAE Technical Report TR83007**, January 1983
5. A Simpson, The Use of Stodola Modes in Rotor Blade Aeroelastic Studies, **Proceedings of the 16th European Rotorcraft Forum**, Paper No II.3.4, Glasgow, Scotland. Sept 1990
6. G D Padfield and R W Du Val, Simulation Model Validation, to be published in **AGARD Lecture Series 178**, 1991
7. D M Pitt and D A Peters, Theoretical Prediction of Dynamic Inflow Derivatives, **Vertica**, Volume 5, pp 21-34, 1981
8. J Riley, G Padfield and J Smith, Estimation of Rotor Blade Deformation from the Measurement of Pressures and Strains in Flight, **Proceedings of the 14th European Rotorcraft Forum**, Paper No 110, Milan, Italy. Sept. 1988
9. G P Turner, Consistency Analysis of Helicopter Flight Test Data, **RAE Technical Memorandum (in preparation)**

10. S S Houston and P C Tarttelin, Theoretical and Experimental Correlation of Helicopter Aeromechanics in Hover, **Proceedings of the 45th Annual Forum of the American Helicopter Society**, Boston, USA. May 1989
11. S S Houston and C G Black, On the Identifiability of Helicopter Models Incorporating Higher Order Dynamics, **Proceedings of the 15th European Rotorcraft Forum**, Amsterdam, The Netherlands. Sept 1989
12. R W Du Val, O Bruhis, J M Harrison and J W Harding, Flight Simulation Model Validation Procedure, a Systematic Approach, **Vertica**, Volume 13, pp311-326, 1989
13. D G Thomson and R Bradley, Validation of Helicopter Mathematical Models by Comparison of Data from Nap-of-the-earth Flight Tests and Inverse Simulations, **Proceedings of the 14th European Rotorcraft Forum**, Paper No 78, Milan, Italy. Sept 1988
14. D A Peters and Ninh HaQuang, Dynamic Inflow for Practical Applications, **Journal of the American Helicopter Society**, Volume 33 #4, October 1988
15. R T N Chen, A Survey of Nonuniform Inflow Models for Rotorcraft Flight Dynamics and Control Applications, **Proceedings of the 15th European Rotorcraft Forum**, Paper No 64, Amsterdam, The Netherlands. Sept 1989

© Crown Copyright, 1991

Configuration	θ_0	θ_{1s}	θ_{1c}	β_0	β_{1s}	β_{1c}
Puma* (Flight)	0.2143	0.0438	0.0093	0.0621	0.0081	-0.056
Helistab	0.2537	0.0543	0.0092	0.0792	0.0116	-0.054
Glauert Inflow Simple Loads	"	"	"	0.0792	0.0115	-0.054
Pitt-Peters Inflow Simple Loads	"	"	"	0.0792	0.0129	-0.053
Pitt-Peters Inflow Mach Corrected Loads	"	"	"	0.0893	0.0126	-0.054

* Aircraft mass 5472 kg. OAT 15-20 °C

Table 1 : Comparison of simulation and flight trim condition



Figure 1 : The Bedford Research Puma

SCHEMATIC OF QUICK HOP MANOEUVRE

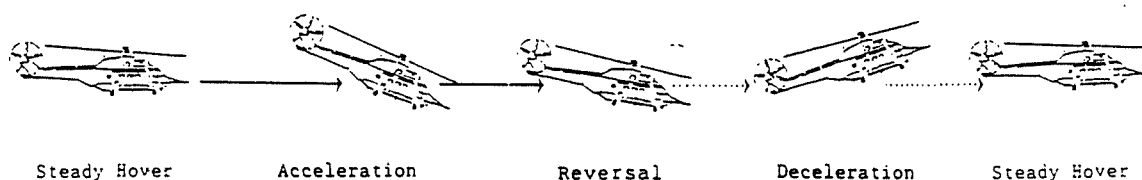


Figure 2 : Profile of the quickhop manoeuvre

PUMA.F003.EVENT191						
TAS (kn)	ROT SPEED	TEMP (C)	ALT (ft)	A/C MASS (kg)	MU	TC
0.00	264.74	20.00	-1093.00	5472.00	0.00000	0.06148

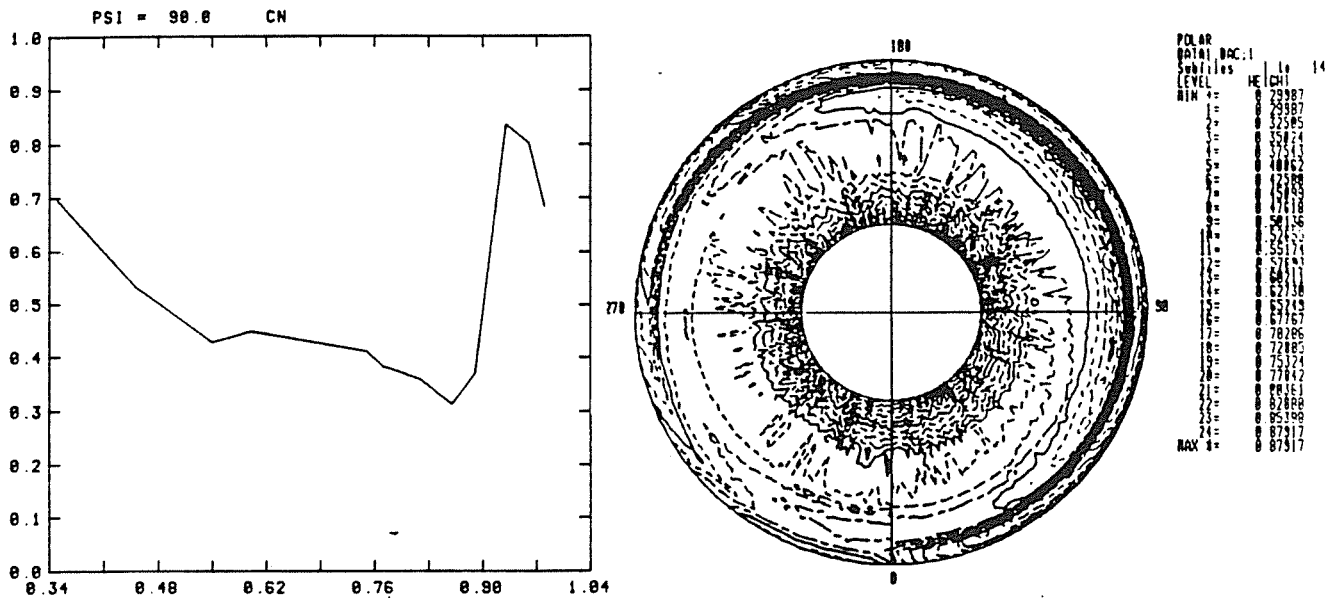


Figure 3 : Typical RIBAN output : Polar and Spanwise plots of C_N

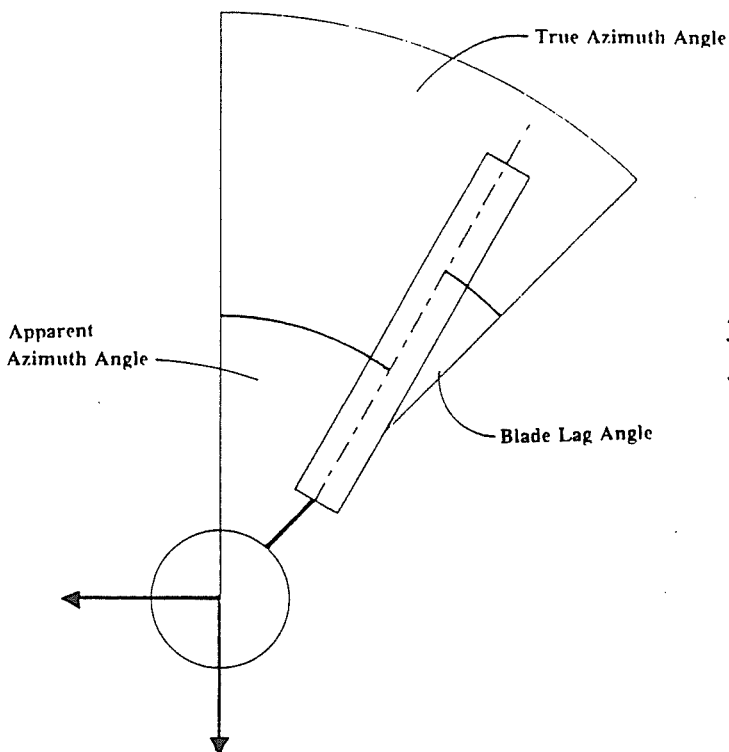


Figure 4 : Relationship between apparent and true blade azimuth

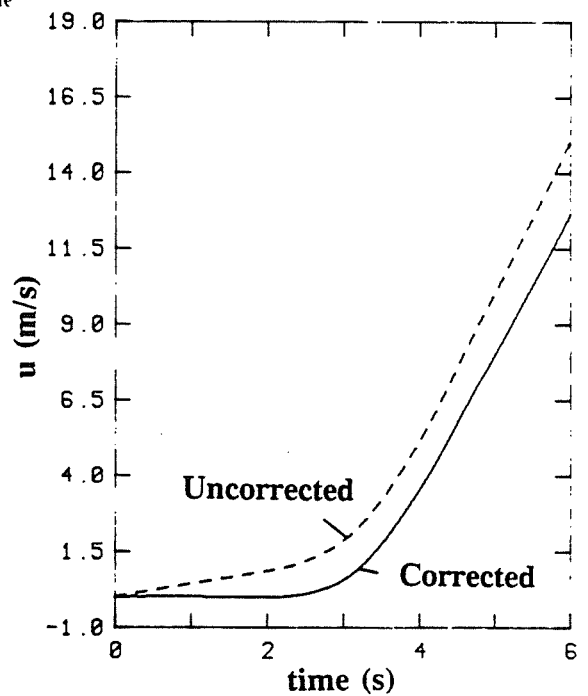


Figure 5 : Removal of integrated bias error on reconstructed velocity trace

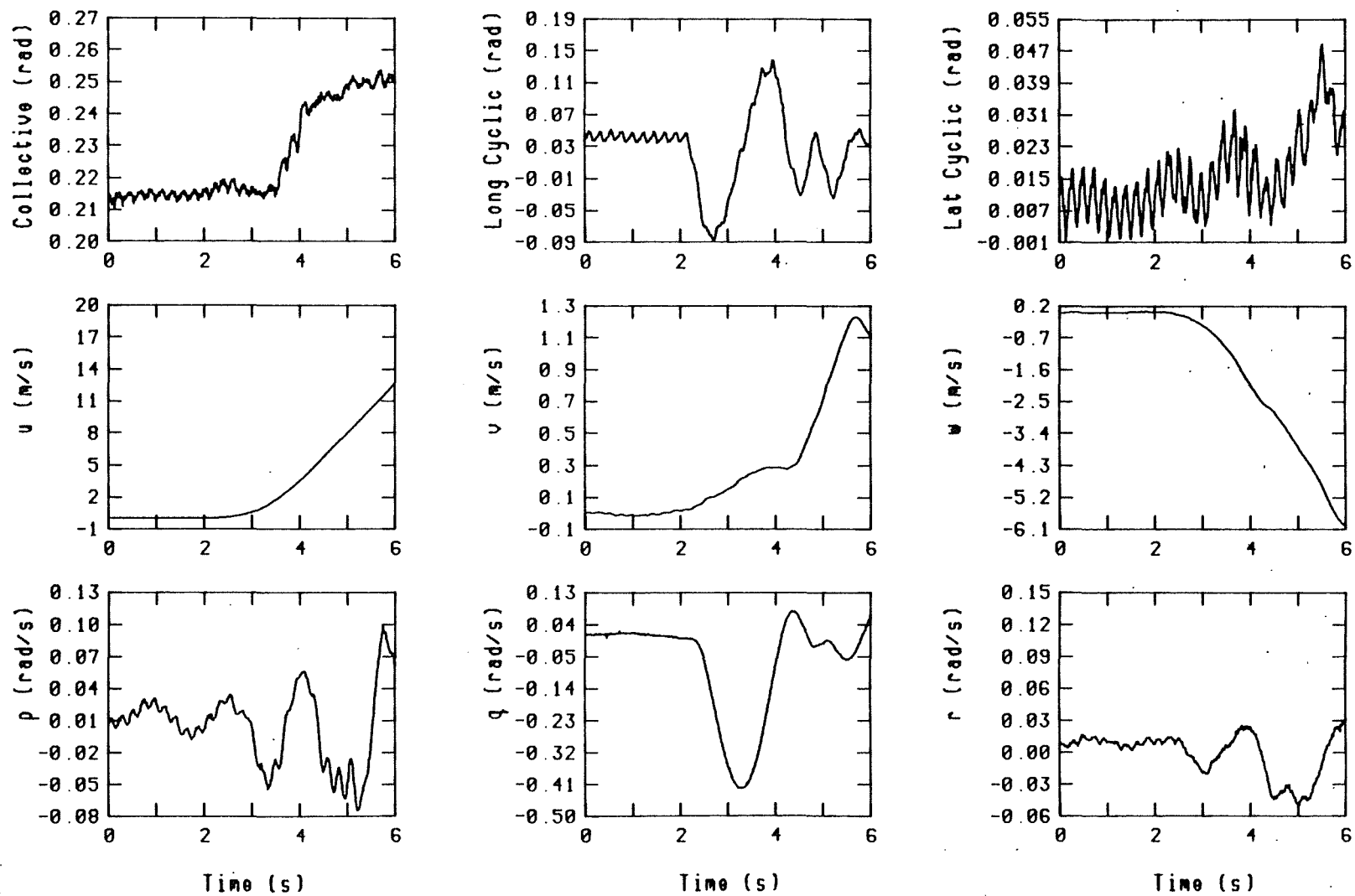


Figure 6 : Rotor controls and fuselage rates, initial 6 seconds of Event 19

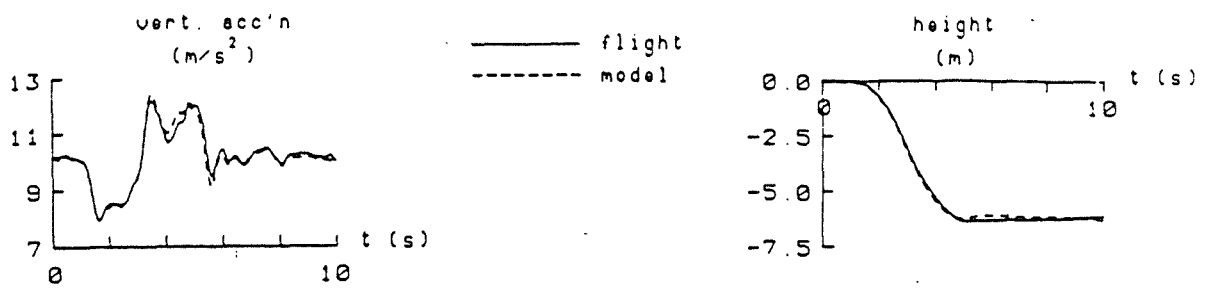


Figure 7 : Bob-up and remask manoeuvre (from Reference 10)

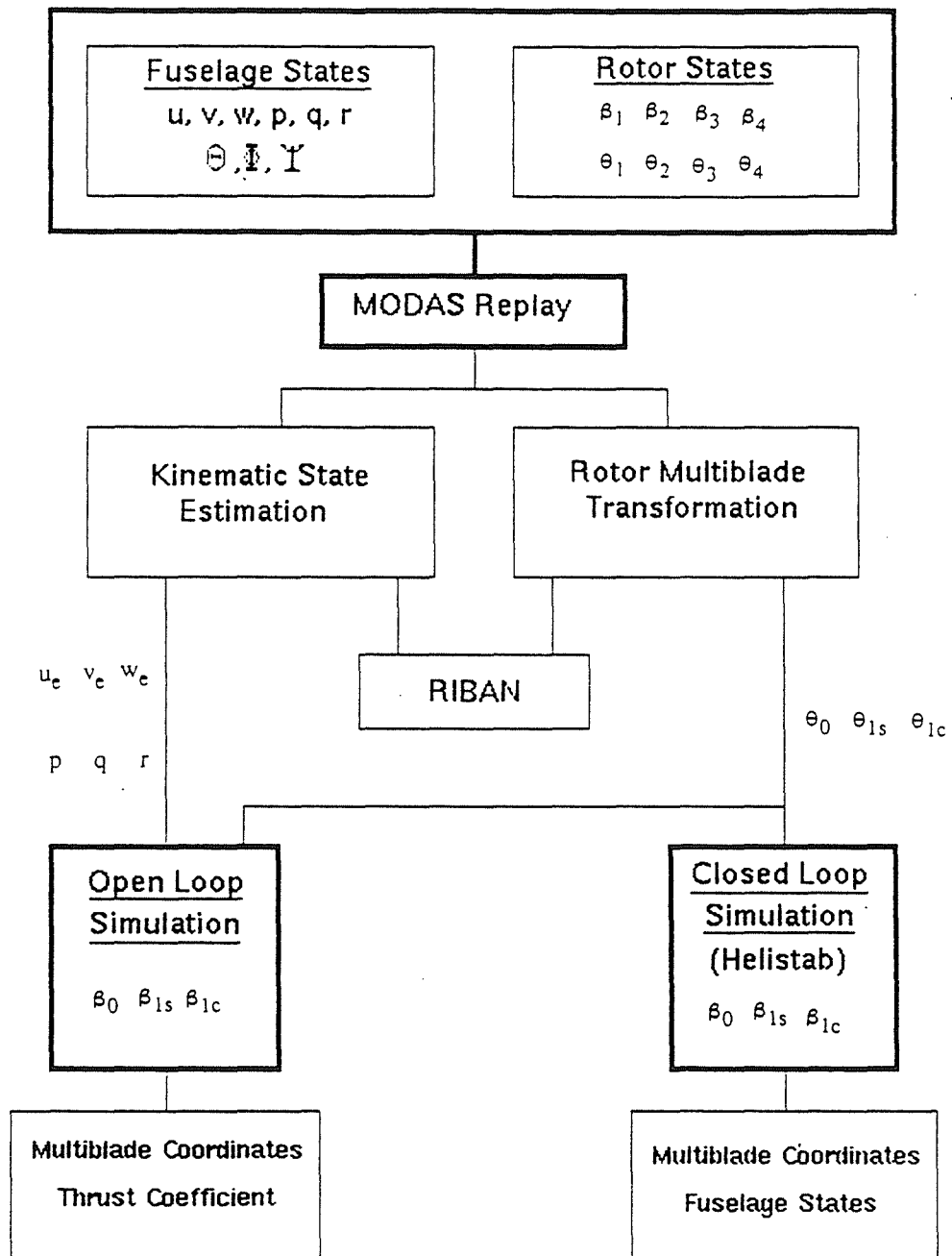


Figure 8 : Flow of data from flight recorder to simulation

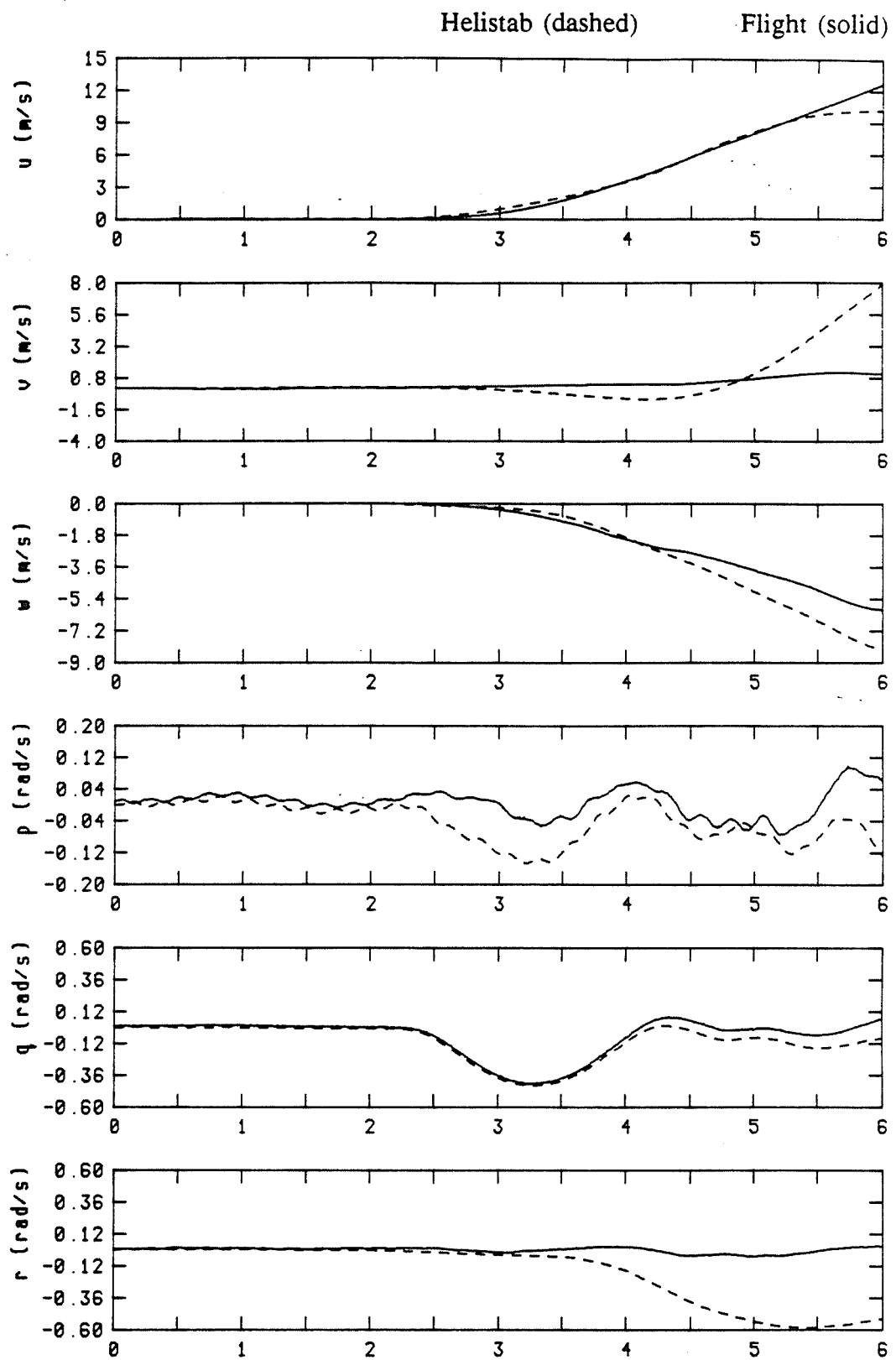


Figure 9 : Fuselage Rates : Helistab vs Flight, Event 19

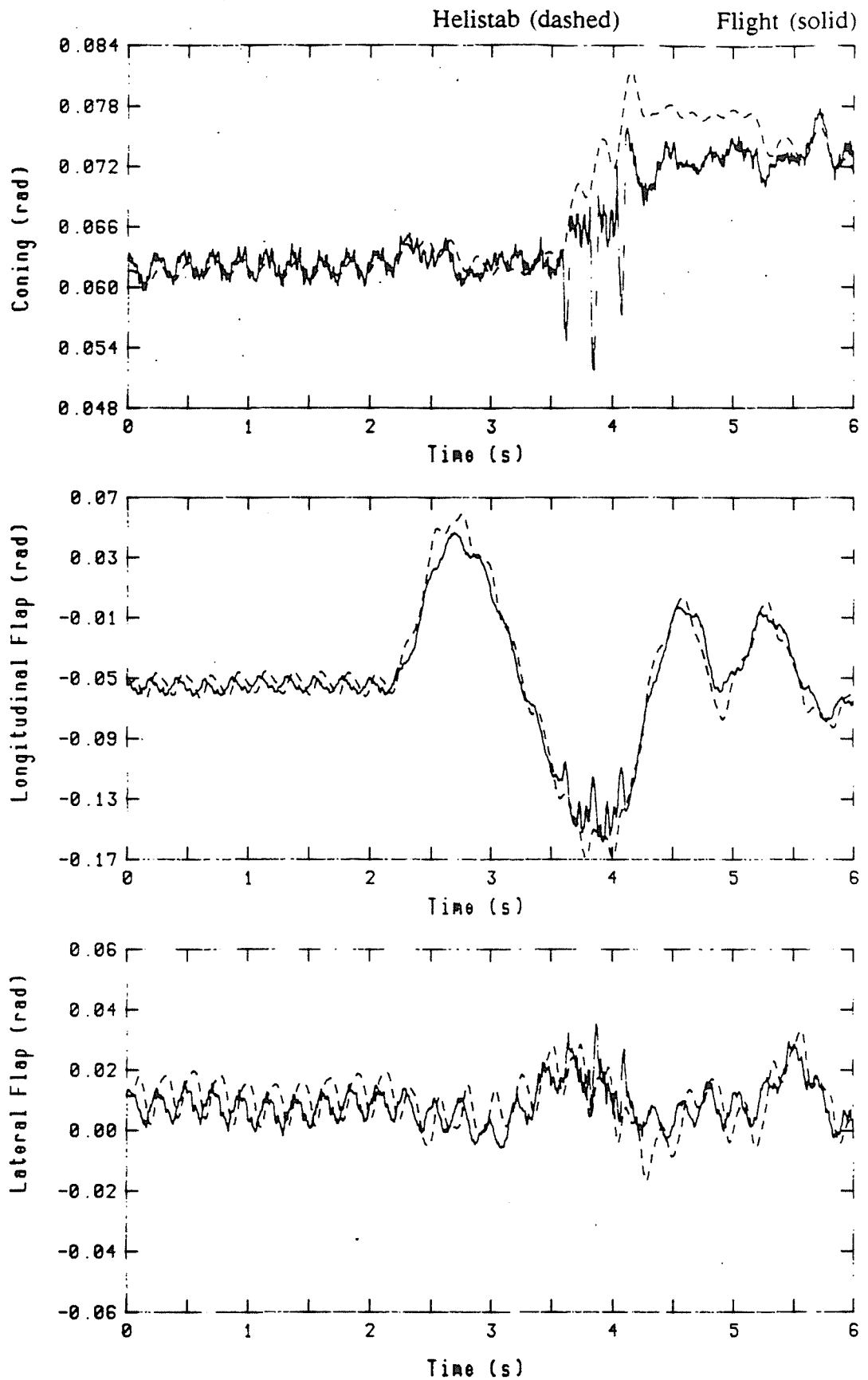


Figure 10: Multiblade coordinates : Helistab vs Flight, Event 19

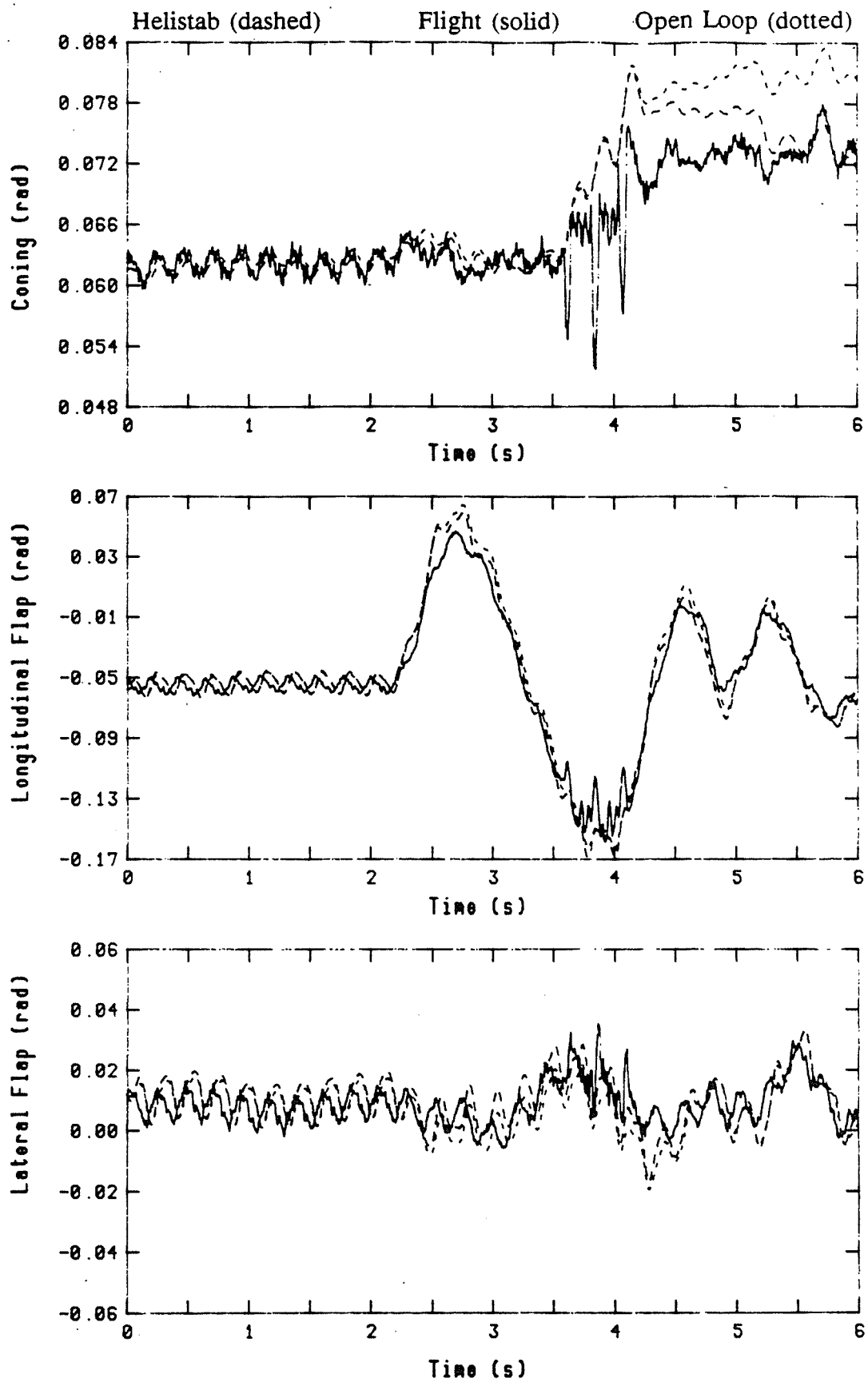


Figure 11: Open- and closed-loop simulation vs Flight, Event 19

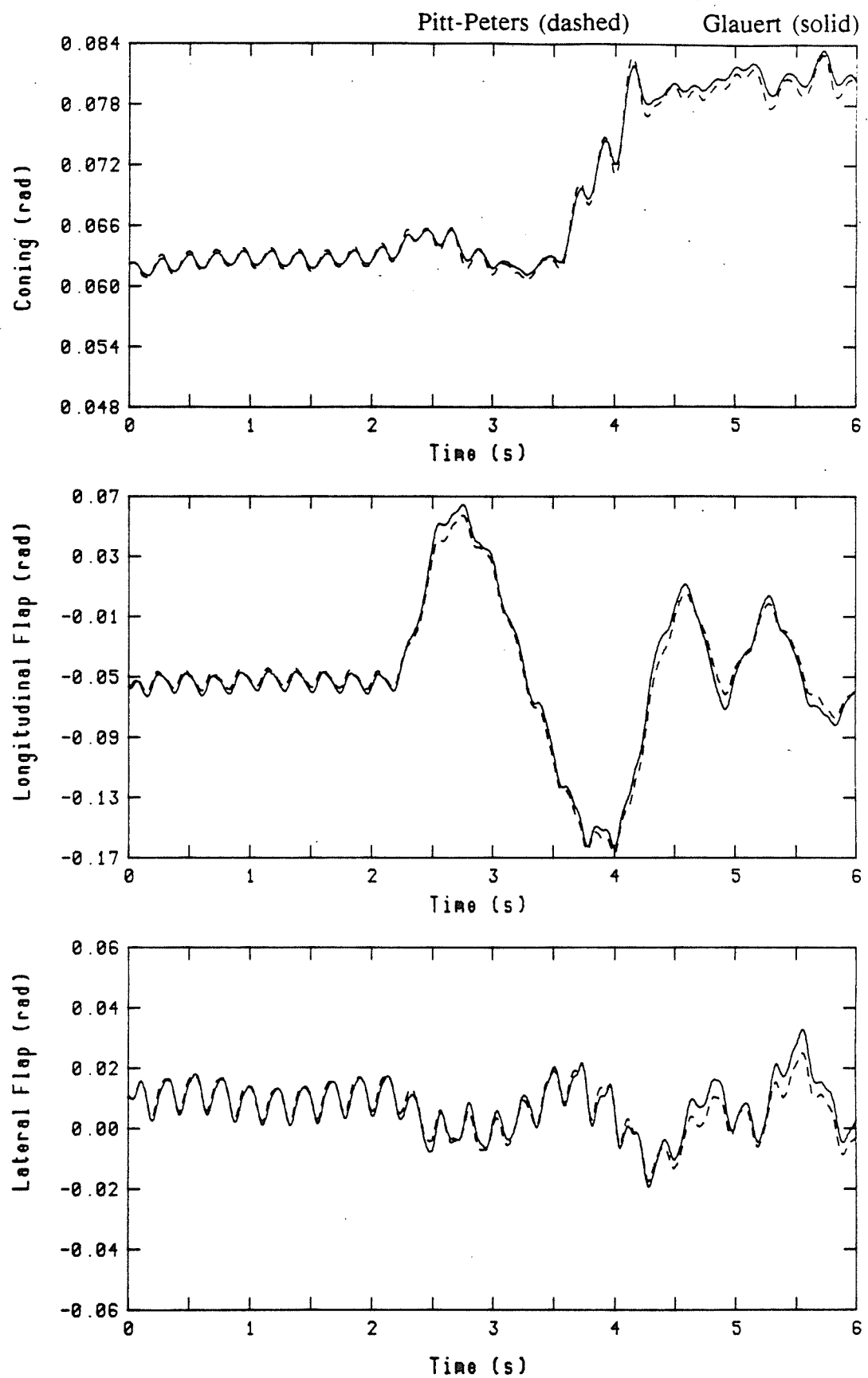


Figure 12: Open loop simulation with and without dynamic inflow

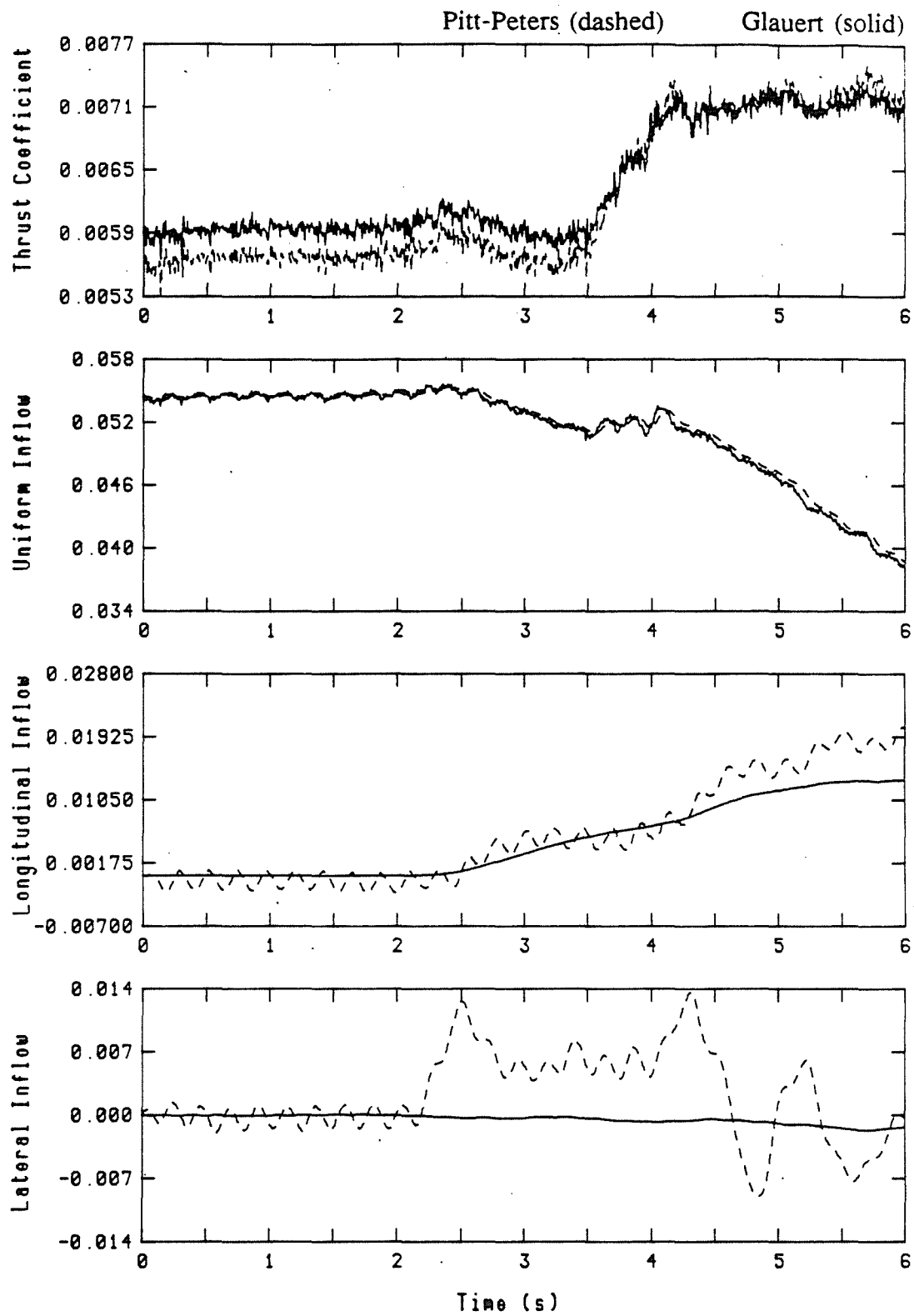


Figure 13: Inflow and thrust coefficients with and without dynamic inflow

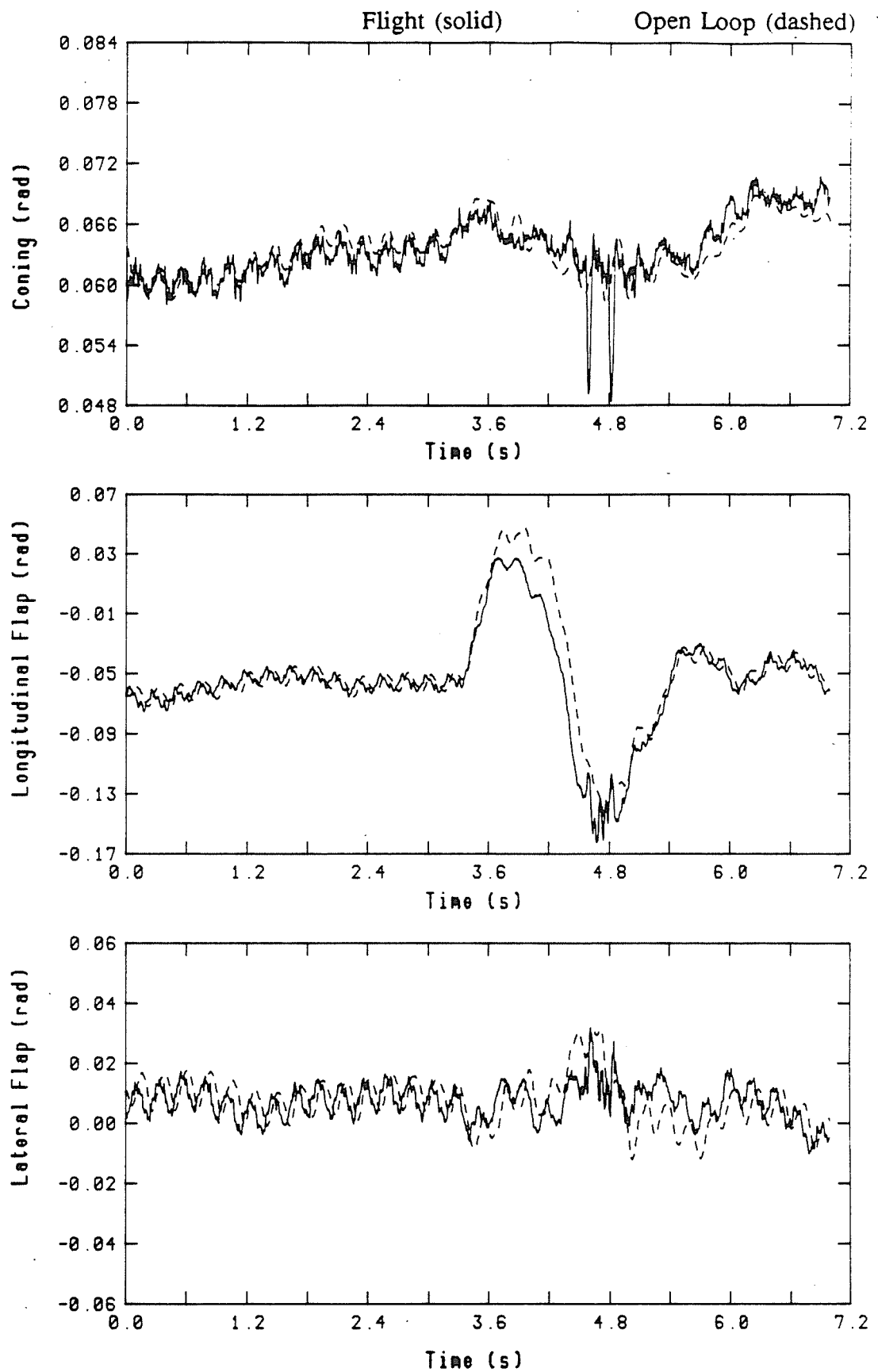


Figure 14: Multiblade coordinates, Open-loop vs Flight, Event 18

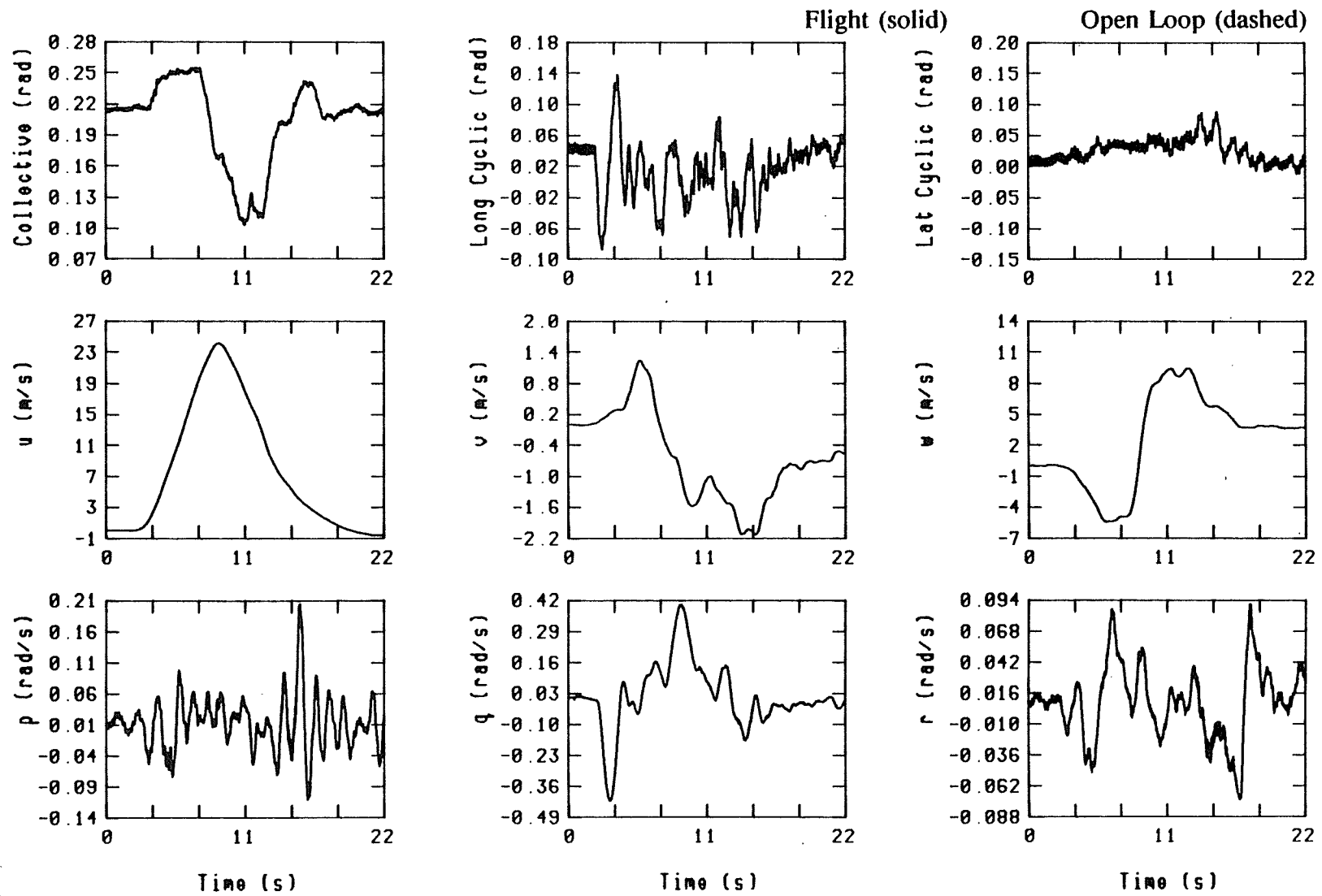


Figure 15: Rotor controls and body rates, all 22 seconds of Event 19

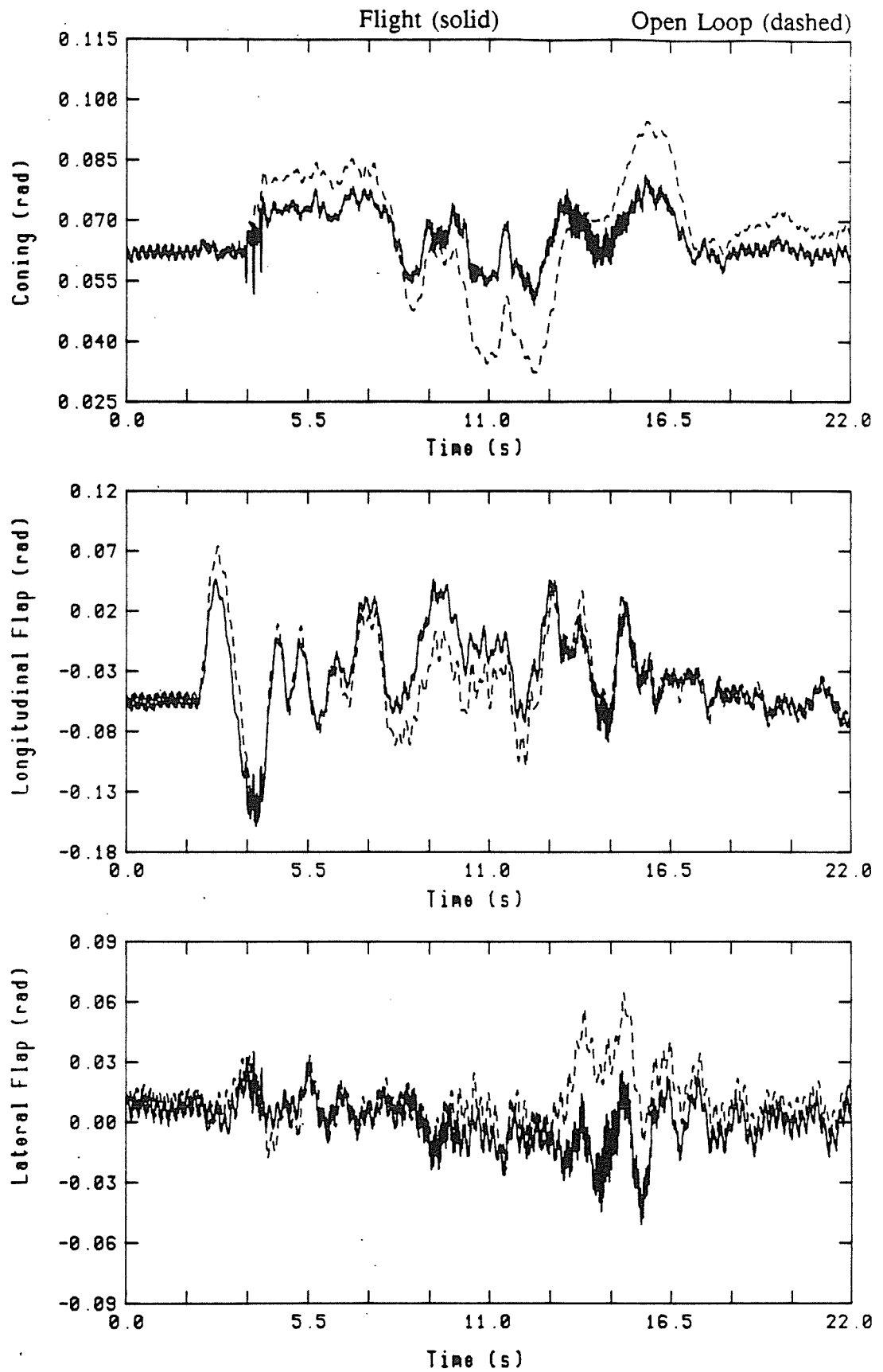


Figure 16: Open-loop simulation vs Flight for all of Event 19

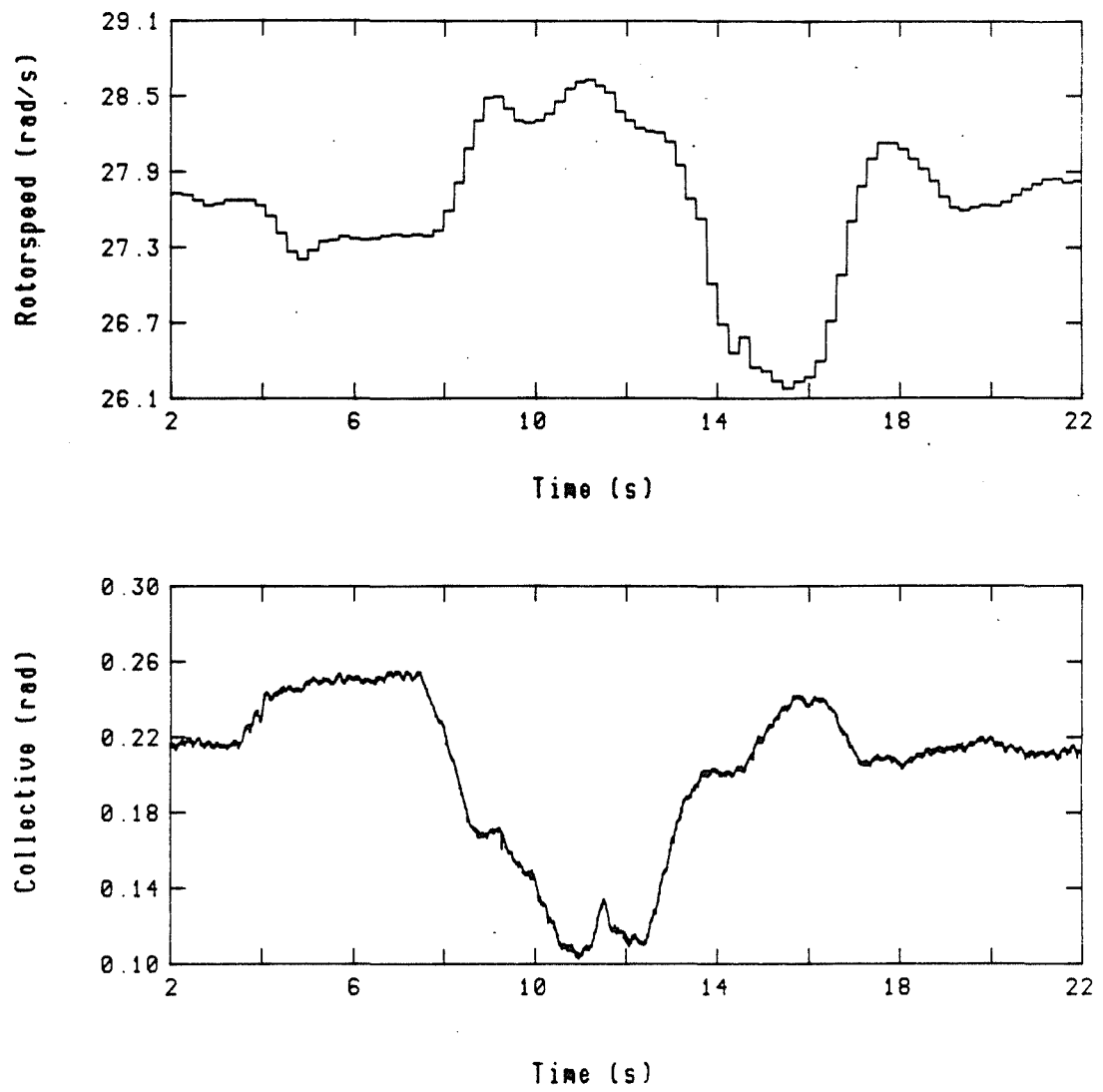


Figure 17: Variation of Puma rotorspeed during Event 19

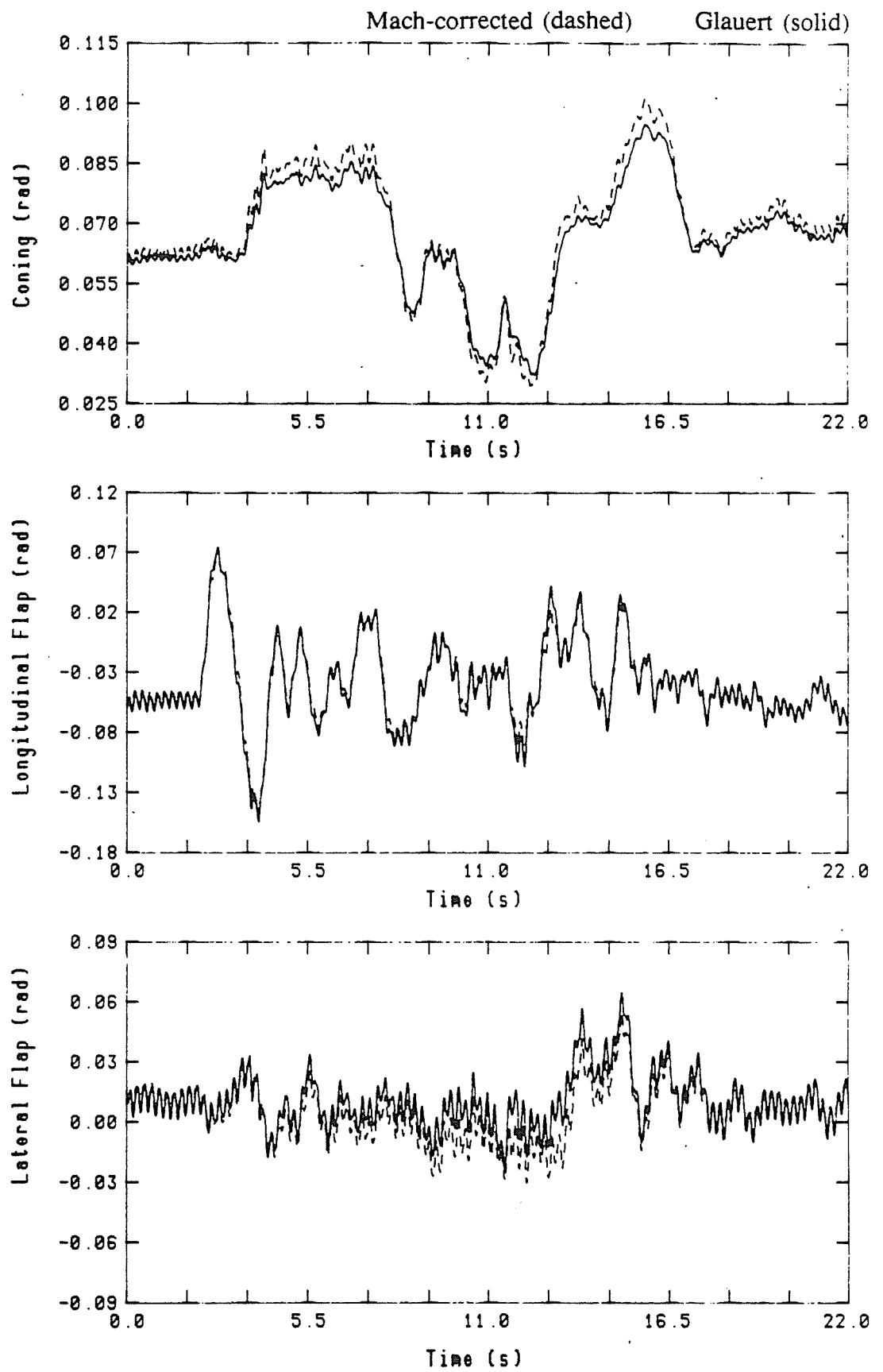


Figure 18: Mach Corrected, Dynamic Inflow model vs simple Glauert